

Hidden SUSY at the LHC: the light higgsino-world scenario and the role of a lepton collider

Howard Baer^a, Vernon Barger^b and Peisi Huang^b

^a*Dept. of Physics and Astronomy, University of Oklahoma, Norman, OK 73019, USA*

^b*Dept. of Physics, University of Wisconsin, Madison, WI 53706, USA*

E-mail: baer@nhn.ou.edu, barger@pheno.wisc.edu, phuang7@wisc.edu

ABSTRACT: While the SUSY flavor, CP and gravitino problems seem to favor a very heavy spectrum of matter scalars, fine-tuning in the electroweak sector prefers low values of superpotential mass μ . In the limit of low μ , the two lightest neutralinos and light chargino are higgsino-like. The light charginos and neutralinos may have large production cross sections at LHC, but since they are nearly mass degenerate, there is only small energy release in three-body sparticle decays. Possible dilepton and trilepton signatures are difficult to observe after mild cuts due to the very soft p_T spectrum of the final state isolated leptons. Thus, the higgsino-world scenario can easily elude standard SUSY searches at the LHC. It should motivate experimental searches to focus on dimuon and trimuon production at the very lowest $p_T(\mu)$ values possible. If the neutralino relic abundance is enhanced via non-standard cosmological dark matter production, then there exist excellent prospects for direct or indirect detection of higgsino-like WIMPs. While the higgsino-world scenario may easily hide from LHC SUSY searches, a linear e^+e^- collider or a muon collider operating in the $\sqrt{s} \sim 0.5 - 1$ TeV range would be able to easily access the chargino and neutralino pair production reactions.

KEYWORDS: Supersymmetry Phenomenology, Supersymmetric Standard Model, Large Hadron Collider.

1. Introduction

The well-known instability of the scalar sector of the Standard Model (SM) to quadratic divergences is elegantly solved by the introduction of supersymmetry (SUSY)[1]. In the case of the Minimal Supersymmetric Standard Model (MSSM) with soft SUSY breaking (SSB) terms, the divergences in the scalar sector are rendered to merely logarithmic. Interplay between the electroweak sector and the SUSY partners suggests the superpartner masses should exist at or around the TeV scale to avoid re-introduction of fine-tuning.

While the MSSM may be very appealing, it does suffer several pathologies. Unfettered soft SUSY breaking terms lead to large rates for flavor-changing neutral current processes and CP violation[2]. Inclusion of grand unified theories with SUSY may lead to unacceptably high rates for proton decay[3]. And in gravity-mediated SUSY breaking models (SUGRA), gravitino production followed by late-time gravitino decays in the early universe are in conflict with the successful picture of Big Bang nucleosynthesis (BBN) unless re-heat temperatures after inflation are limited to $T_R \lesssim 10^5$ GeV[4]. The latter bound is in conflict with appealing baryogenesis models such as thermal[5] (or non-thermal[6]) leptogenesis, which require $T_R \gtrsim 2 \times 10^9$ GeV (10^6 GeV).

A common solution to the above four problems is to push the SUSY matter scalars into the multi-TeV regime[7]. The heavy scalars thus suppress loop-induced flavor and CP violating processes, and suppress proton decay rates. If the multi-TeV scalars derive from a SUGRA model with a simple form for the Kähler potential, then the gravitino mass $m_{3/2}$ is also expected to exist in the multi-TeV range. By pushing $m_{3/2}$ into the 10-50 TeV range, the gravitino lifetime can be reduced to $\tau_{3/2} \lesssim 1$ second, so the gravitino decays shortly before BBN begins, this solving the gravitino problem[8].

At first glance, multi-TeV gravitino and scalar masses seem in conflict with SUSY electroweak fine-tuning. The possible SUSY electroweak fine-tuning arises from minimization of the scalar potential after electroweak symmetry breaking. Here, the tree-level electroweak breaking conditions are familiarly written as[9]

$$B\mu = \frac{(m_{H_u}^2 + m_{H_d}^2 + 2\mu^2) \sin 2\beta}{2}, \quad \text{and} \quad (1.1)$$

$$\mu^2 = \frac{m_{H_d}^2 - m_{H_u}^2 \tan^2 \beta}{(\tan^2 \beta - 1)} - \frac{M_Z^2}{2}, \quad (1.2)$$

where B is the bilinear SSB term and $m_{H_u}^2$ and $m_{H_d}^2$ are the up and down Higgs SSB masses evaluated at the weak scale, μ is the superpotential Higgs mass term and $\tan \beta$ is the ratio of Higgs field vevs: $\tan \beta = \frac{v_u}{v_d}$.

A measure of fine-tuning

$$\Delta_i \equiv \left| \frac{\partial \log M_Z^2}{\partial \log a_i} \right| \quad (1.3)$$

was advocated in Ref. [10]. More sophisticated measures were advocated in Ref's [11], while in Ref. [12], the μ parameter itself is taken as a measure of fine-tuning: the latter paper requires $|\mu| \lesssim 1$ TeV to avoid too much fine-tuning. This measure motivates the well-known hyperbolic branch/ focus point (HB/FP) region of minimal supergravity (mSUGRA

or CMSSM) as allowing for heavy scalars with low μ value and low fine-tuning[12, 13]. A virtue of the HB/FP region is that multi-TeV scalars can co-exist with apparent low levels of electroweak fine-tuning.

In this paper, we will consider supersymmetric models with large, multi-TeV scalar masses, but with low, sub-TeV superpotential μ term. We consider the case with intermediate range gaugino masses. This scenario, with

$$|\mu| \ll m_{\text{gauginos}} \ll m_{\text{scalars}}, \quad (1.4)$$

has been dubbed “higgsino-world” by Kane[14], and leads to a sparticle mass spectrum with a light higgsino-like chargino \widetilde{W}_1 and two light higgsino-like neutralinos \widetilde{Z}_1 and \widetilde{Z}_2 . In models with gaugino mass unification at M_{GUT} , then the state \widetilde{Z}_3 will be mainly bino-like, while \widetilde{Z}_4 and \widetilde{W}_2 will be wino-like.

While the higgsino-world scenario seems highly appealing due to its ability to reconcile multi-TeV scalars and gravitinos with low electroweak fine-tuning, it has perhaps fallen out of favor for two reasons. First, higgsino-world leads to a very low thermal relic density of neutralinos, not at all in accord with measurements from WMAP and other experiments which require[15]

$$\Omega_{\text{DM}} h^2 = 0.1123 \pm 0.0035 \quad \text{at 68\% CL.} \quad (1.5)$$

Second, higgsino-world scenarios are not easily realized in the paradigm mSUGRA/CMSSM framework, since elevating scalar masses into the multi-TeV region for a given value of GUT scale gaugino mass $m_{1/2}$ pushes one beyond the HB/FP region into a portion of parameter space where radiative EWSB is not realized under the assumption of universal scalar masses m_0 at M_{GUT} .

Pertaining to the dark matter issue, a number of recent works have emphasized that the standard picture of a thermal SUSY WIMP as dark matter is subject to very high fine-tuning[16]. Furthermore, non-standard cosmologies have many desirable features, and may even be favored by string theoretic constructions. For instance, Kane *et al.* have shown[17] that at least one moduli field in string theory should maintain a mass at or around the 10 TeV scale. Such moduli fields can be produced via coherent oscillations in the early universe, and decay into WIMPs, thereby augmenting the WIMP abundance[18], or they can decay into SM particles, thus generating entropy and diluting the WIMP abundance. Gelmini *et al.* have shown in this case that SUSY models with *any* value—either too high or too low—of thermal WIMP abundance may give rise to the measured CDM abundance via the enhancement or diminution due to scalar field (moduli) decays[19]. In particular, for higgsino-world with too low a thermal WIMP abundance, the light higgsino abundance can be enhanced by moduli decays, leading to the correct abundance of higgsino-like WIMPs.

Alternatively, in SUSY models wherein the strong CP problem is solved by the introduction of Peccei-Quinn-Weinberg-Wilczek[20] invisible axion[21, 22], one must introduce an axion supermultiplet, which contains an R -parity even spin-0 saxion $s(x)$, along with an R -parity odd spin- $\frac{1}{2}$ axino $\tilde{a}(x)$, in addition to the light pseudoscalar axion field $a(x)$. In models such as these, with a TeV-scale axino and a higgsino-like neutralino as LSP, the \widetilde{Z}_1 abundance can be augmented by axino production and subsequent re-annihilation at

temperatures above BBN but below neutralino freeze-out[23]. Depending on the various PQMSSM model parameters, the CDM consists of an axion/neutralino admixture, where either the axion or the neutralino can dominate the abundance[24].

A third modification of the thermal WIMP abundance may also occur: a model with a supposed underabundance of neutralino dark matter may enjoy enhancement of the relic DM abundance due to thermal gravitino production[25] followed by cascade decays to the LSP state[26, 27].

Pertaining to the issue of higgsino-world being difficult to realize in the paradigm mSUGRA model, we note that it is easily realized in models with non-universal GUT scale Higgs masses (NUHM)[28]. In fact, in GUT models such as $SO(10)$, the matter supermultiplets live in the 16-dimensional spinor representation, while Higgs superfields live in 10 or other dimensional multiplets. In such models, there is little reason to expect matter-Higgs SSB universality at M_{GUT} .

For the above reasons, we feel that it may be opportune to reconsider the higgsino-world scenario, and whether such a scenario would be visible to LHC SUSY searches. Toward this end, we discuss in Sec. 2 the higgsino-world parameter space and expected mass spectra. In Sec. 3, we present calculations of the standard thermal neutralino abundance in the higgsino-world scenario, and discuss its direct and indirect detection in the case where non-standard cosmological processes augment the relic higgsino abundance. In Sec. 4, we evaluate the dominant sparticle production cross sections for the lighter matter states at the LHC and calculate their branching fractions. While higgsino production cross sections occur at possibly observable levels, the compressed spectra lead to sparticle decays with very low energy release, and very soft detectable particles. To the best of our knowledge, higgsino-world SUSY can effectively elude standard SUSY searches for jets plus missing E_T (MET), and also for isolated multi-leptons+ MET at LHC7 (LHC at $\sqrt{s} = 7$ TeV) with $\sim 10 \text{ fb}^{-1}$ of integrated luminosity. In Sec. 5, we discuss higgsino-world signatures at a TeV scale lepton collider such as ILC or a muon collider (MC). In Sec. 6, we present our final discussion and conclusions.

2. Higgsino-world parameter space and mass spectra

We will adopt the Isajet 7.81 program for SUSY particle mass spectrum generation[30]. To generate spectra in higgsino-world scenario, we will adopt the Isasugra non-universal Higgs mass parameter space (NUHM2):

$$m_0, m_{1/2}, A_0, \tan\beta, \mu, m_A. \quad (2.1)$$

In the above parameter space, m_0 , $m_{1/2}$ and A_0 are the usual GUT scale parameters, although here m_0 is reserved only for matter scalars, and not Higgs scalar soft masses. The two additional parameters μ and m_A are stipulated at the weak scale, and are used to solve for the weak scale values of $m_{H_u}^2$ and $m_{H_d}^2$. These latter parameters are run from the weak to GUT scale, and their GUT scale values are determined by enforcing the input weak scale values of μ and m_A . We will take $m_0 \sim m_{\tilde{G}}$ to be in the multi-TeV range, so that we obtain a decoupling solution to the SUSY flavor, CP, p -decay and gravitino problems.

parameter	HW150	HW300
m_0	5000	5000
$m_{1/2}$	800	800
A_0	0	0
$\tan \beta$	10	10
μ	150	300
m_A	800	800
$m_{\tilde{g}}$	2004.9	2004.2
$m_{\tilde{u}_L}$	5171.5	5171.4
$m_{\tilde{t}_1}$	3240.2	3243.8
$m_{\tilde{b}_1}$	4267.8	4269.4
$m_{\tilde{e}_R}$	4869.4	4870.1
$m_{\tilde{W}_2}$	672.7	675.4
$m_{\tilde{W}_1}$	156.3	310.5
$m_{\tilde{Z}_4}$	688.2	691.0
$m_{\tilde{Z}_3}$	356.3	366.9
$m_{\tilde{Z}_2}$	158.9	311.4
$m_{\tilde{Z}_1}$	142.7	283.2
m_h	120.1	120.1
$\sigma(LHC7)$	1055 fb	63.5 fb
$\Omega_{\tilde{Z}_1}^{std} h^2$	0.008	0.03
$BF(b \rightarrow s\gamma)$	3.5×10^{-4}	3.5×10^{-4}
$\sigma^{SI}(\tilde{Z}_1 p)$ (pb)	1.0×10^{-8}	3.1×10^{-8}
$\langle \sigma v \rangle _{v \rightarrow 0}$ (cm ³ /sec)	0.28×10^{-24}	0.09×10^{-24}
$v_H^{(1)}$	0.98	0.90

Table 1: Input parameters and masses in GeV units for two higgsino-world scenario benchmark points HW150 and HW300, with $\mu = 150$ and 300 GeV, respectively.

Thus, the parameters m_0 and also A_0 and m_A will be largely irrelevant for our analysis. The main parameter space dependence will arise from just varying μ and $m_{1/2}$. Since we are interested in the light higgsino-world scenario, with $\mu \ll M_i$ (where M_i are the weak scale gaugino masses), the parameter $\tan \beta$, which induces gaugino-higgsino mixing, will also not be terribly relevant.

The higgsino-world input parameters and mass spectra for two sample benchmark points with $\mu = 150$ and 300 GeV are listed in Table 1. We also take $m_0 = 5000$ GeV, $m_{1/2} = 800$ GeV, $A_0 = 0$, $\tan \beta = 10$ and $m_A = 800$ GeV. The spectra are also shown in Fig. 1 for the higgsino-world case where $\mu = 150$ GeV (HW150).

From Table 1 or Fig. 1, we see that the three states \tilde{W}_1 , \tilde{Z}_1 and \tilde{Z}_2 all have masses clustered around the value of $\mu = 150$ or 300 GeV. These states are dominantly higgsino-like. The weak scale gaugino masses $M_1 \sim 352$ GeV and $M_2 \sim 638$ GeV for the two cases, so that \tilde{Z}_3 is bino-like and \tilde{W}_2 and \tilde{Z}_4 are wino-like. The squarks and sleptons all are

decoupled, with masses in the multi-TeV range, since $m_0 = 5$ TeV. The $\tilde{Z}_2 - \tilde{Z}_1$ mass gap is just 16.2 GeV and 28.2 GeV, respectively, for the two cases. We also show the higgsino fraction of the lightest neutralino: $v_H = \sqrt{v_1^{(1)2} + v_2^{(1)2}}$ where $v_1^{(i)}$ is the higgsino \tilde{h}_u^0 content and $v_2^{(i)}$ is the higgsino \tilde{h}_d^0 content of neutralino \tilde{Z}_i in the notation of Ref. [9]. Here, the value of v_H is 0.98 for HW150 and 0.9 for HW300. Increasing μ to 500 GeV, using the same choice of other model parameters, decreases $v_H \sim 0.21$, so that in this case the lightest neutralino is no longer dominantly higgsino-like, but rather of mixed higgsino-bino variety. We also see from Table 1 that the standard thermal neutralino abundance is $\Omega_{\tilde{Z}_1}^{std} h^2 \sim 0.008$ and 0.03, respectively, *i.e.* well below the WMAP-measured CDM abundance.

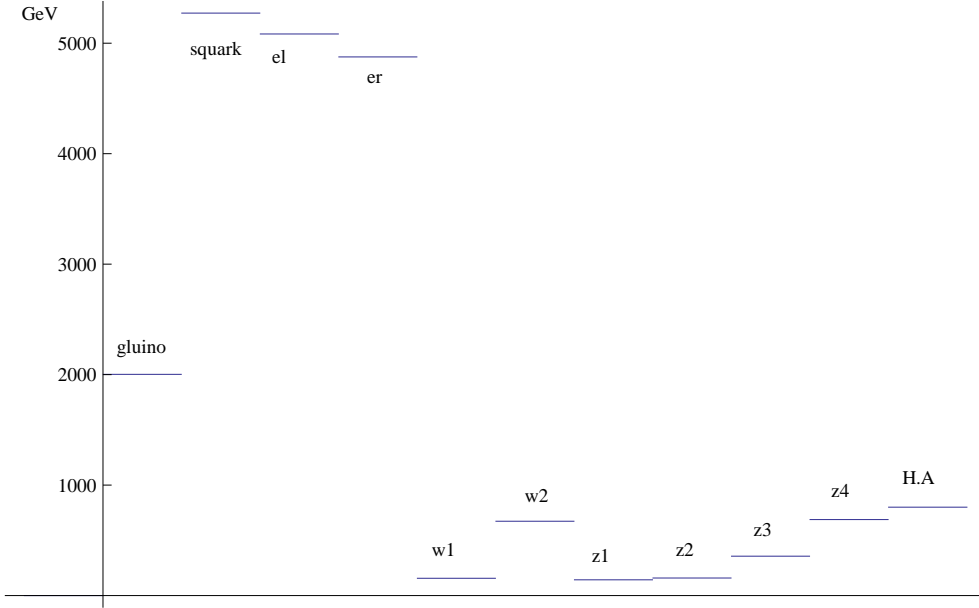


Figure 1: Sparticle mass spectra for a light higgsino world scenario with $\mu = 150$ GeV, $m_A = 800$ GeV, $m_0 = 5000$ GeV, $m_{1/2} = 600$ GeV, $A_0 = 0$ and $\tan \beta = 10$. We take $m_t = 173.3$ GeV.

In Fig. 2, we show color-coded contours of the higgsino fraction v_H of the lightest neutralino \tilde{Z}_1 in the μ *vs.* $m_{1/2}$ parameter space plane for $m_0 = 5$ TeV, $A_0 = 0$ and $\tan \beta = 10$. The green, yellow and especially red regions contain a lightest neutralino with large higgsino fraction $v_H \gtrsim 0.5$. This region essentially defines the higgsino-world scenario parameter space, which is found at low $|\mu|$ and large $m_{1/2}$. As one enters the blue-shaded region, the \tilde{Z}_1 becomes increasingly bino-like. The unshaded region at low μ is excluded by LEP2 limits on the lightest chargino: $m_{\tilde{W}_1} \lesssim 103.5$ GeV.

In Fig. 3, we show a). the color-coded mass contours of the lightest neutralino \tilde{Z}_1 , and b). the $m_{\tilde{Z}_2} - m_{\tilde{Z}_1}$ mass gap (which is always very close to the value of the $m_{\tilde{W}_1} - m_{\tilde{Z}_1}$ mass gap). In the higgsino-world scenario with low μ and large $m_{1/2}$, we find that $m_{\tilde{Z}_1}$ can drop as low as ~ 90 GeV, where the lower limit comes from the LEP2 constraint on chargino masses. Meanwhile, the mass gap $m_{\tilde{Z}_2} - m_{\tilde{Z}_1}$ drops as low as ~ 10 GeV in the extreme higgsino-world region. Thus, for extreme higgsino-world parameters, we always expect the \tilde{Z}_2 states to decay via three-body modes or loop-suppressed two-body decays

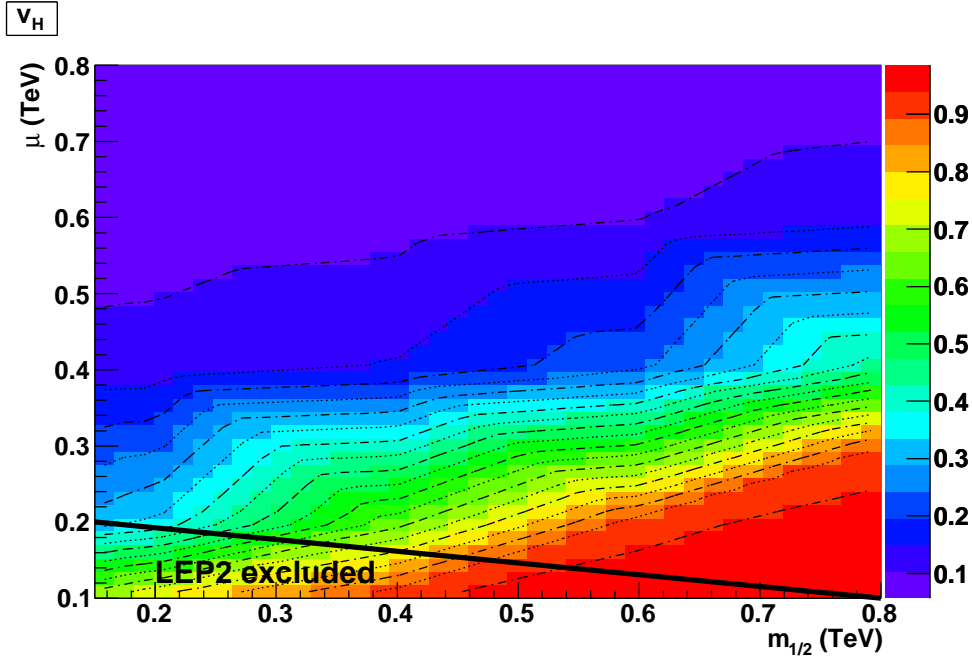


Figure 2: Color-coded contours of higgsino content v_H of the \tilde{Z}_1 in the μ vs. $m_{1/2}$ plane with $m_A = 800$ GeV, $m_0 = 5000$ GeV, $A_0 = 0$ and $\tan\beta = 10$.

such as $\tilde{Z}_2 \rightarrow \tilde{Z}_1 \gamma$ [35]. Two-body decays such as $\tilde{Z}_2 \rightarrow \tilde{Z}_1 Z$ or $\tilde{Z}_1 h$ will always be closed in the higgsino-world scenario.

3. Neutralino relic density and direct detection rates

In the light higgsino-world scenario, if the lightest neutralino is dominantly higgsino-like, then it will sustain large $\tilde{Z}_1 \tilde{Z}_1$ annihilation cross sections into vector boson states ZZ and W^+W^- . This will result in a standard thermal neutralino abundance typically well below WMAP-measured values of $\Omega_{CDM} h^2 \sim 0.11$. In Fig. 4, we show color-coded contours of the standard thermal neutralino abundance $\log_{10} \Omega_{\tilde{Z}_1}^{std} h^2$. We see that indeed in the low μ region $\Omega_{\tilde{Z}_1}^{std} h^2$ is at the $10^{-2.5} - 10^{-1}$ range, where 10^{-1} occurs for mixed higgsino-bino states. Thus, a non-standard cosmology is likely needed to explain the CDM abundance in the higgsino-world scenario. Indeed, many “non-standard” scenarios can be highly motivated by other physics considerations (the presence of TeV-scale moduli in string theory, the axion solution to the strong CP problem \dots), and so may well be more appealing than simple thermal production of WIMPs.

If the higgsino relic abundance is enhanced (say, by moduli decays, or by axino production and decay, or by gravitino production and decay) beyond standard expectations, then a higgsino-like WIMP may well make up the bulk of dark matter. In this case, we present in Fig. 5 color-coded contours of spin-independent neutralino-proton scattering cross section in units of 10^{-9} pb in the μ vs. $m_{1/2}$ plane. The red and yellow shaded regions have $\sigma_{SI}(p\tilde{Z}_1) \gtrsim 30 \times 10^{-9}$ pb, while green-shaded regions have $\sigma_{SI}(p\tilde{Z}_1) \gtrsim 20 \times 10^{-9}$ pb. The

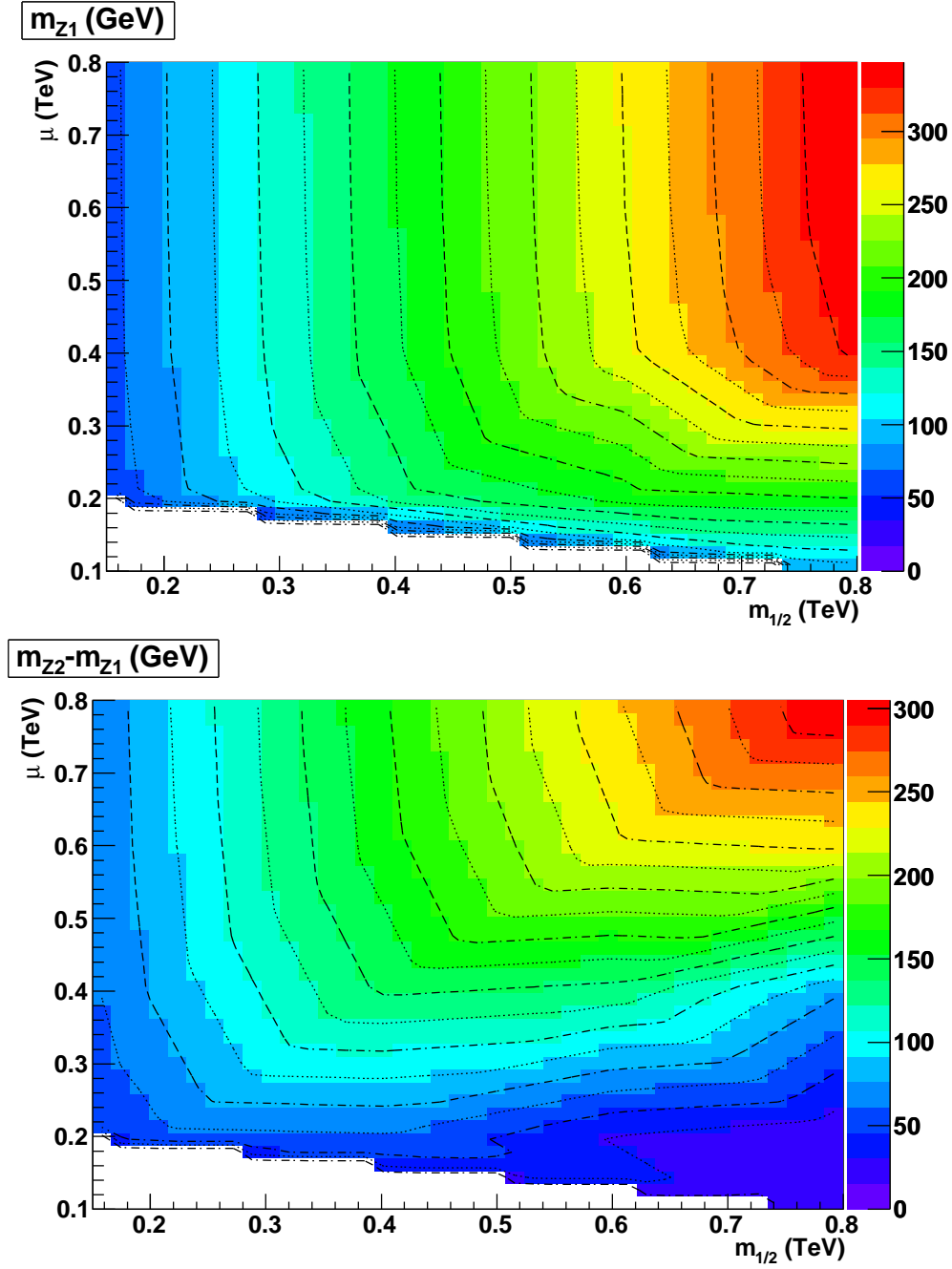


Figure 3: In *a*), we plot contours of $m_{\tilde{Z}_1}$ while in *b*), we plot contours of $m_{\tilde{Z}_2} - m_{\tilde{Z}_1}$ in the μ vs. $m_{1/2}$ plane with $m_A = 800$ GeV, $m_0 = 5000$ GeV, $A_0 = 0$ and $\tan\beta = 10$.

Xenon-100 experiment[36]– for $m_{WIMP} \sim 100 - 200$ GeV–excludes $\sigma_{SI}(\tilde{Z}_1 p) \gtrsim 10^{-8}$ pb, so already a large portion of higgsino-world parameter space is excluded if higgsino-like WIMPs make up all the CDM. It is shown in Ref. [24] that in the case of the Peccei-Quinn augmented MSSM, where an axion-axino-saxion supermultiplet is required to solve the strong CP -problem, that for some ranges of PQMSSM parameters, higgsino-like WIMPs

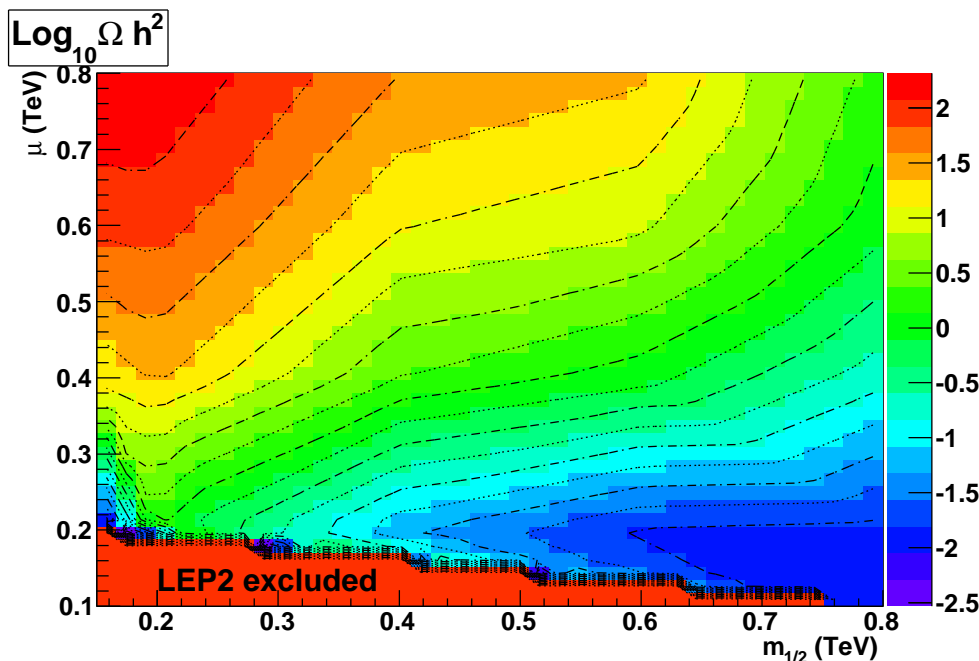


Figure 4: Regions of thermal neutralino abundance in the μ vs. $m_{1/2}$ plane with $m_A = 800$ GeV, $m_0 = 5000$ GeV, $A_0 = 0$ and $\tan\beta = 10$.

could make up virtually all the DM abundance, while for other PQMSSM parameters, (low re-heat temperature T_R or if cosmologically produced axinos decay to neutralinos before neutralino freeze-out), then the CDM abundance may be axion-dominated, while the higgsino abundance maintains its standard relic density. In this latter case, the assumed WIMP abundance would have to be scaled down by a factor of 10-100, and so the higgsino-world scenario would then escape Xenon-100 null-search constraints.

If higgsino-like WIMPs comprise the bulk of dark matter, then it may also be possible to detect them via searches for galactic halo WIMP annihilation into final states containing positrons, anti-protons, gamma-rays or anti-deuterons[37]. In these cases, the WIMP annihilation rate is always proportional to thermally averaged WIMP annihilation cross section times relative velocity, in the limit where $v \rightarrow 0$ (in the galactic halo): $\langle\sigma v\rangle|_{v\rightarrow 0}$. The exact detection rates will also depend on various astrophysical quantities, and details of the detection devices and their backgrounds. Here, we merely present color-coded contours of $\langle\sigma v\rangle|_{v\rightarrow 0}$ in units of $10^{-24} \text{ cm}^3/\text{sec}$. The red-, yellow- and green-shaded regions will typically lead to observable levels of gamma-ray or antimatter detection rates, if higgsino-like WIMPs dominate the CDM relic density. However, in scenarios like the PQMSSM with mixed axion-WIMP dark matter, but with axion domination, these rates will be suppressed due to the low halo abundance of higgsino-like WIMPs. In other PQMSSM cases where the axino \tilde{a} is the LSP[38], then the higgsino-like WIMPs would all have decayed to relic axinos, and no direct or indirect detection signals would be seen (although detection of relic axions would still be possible).

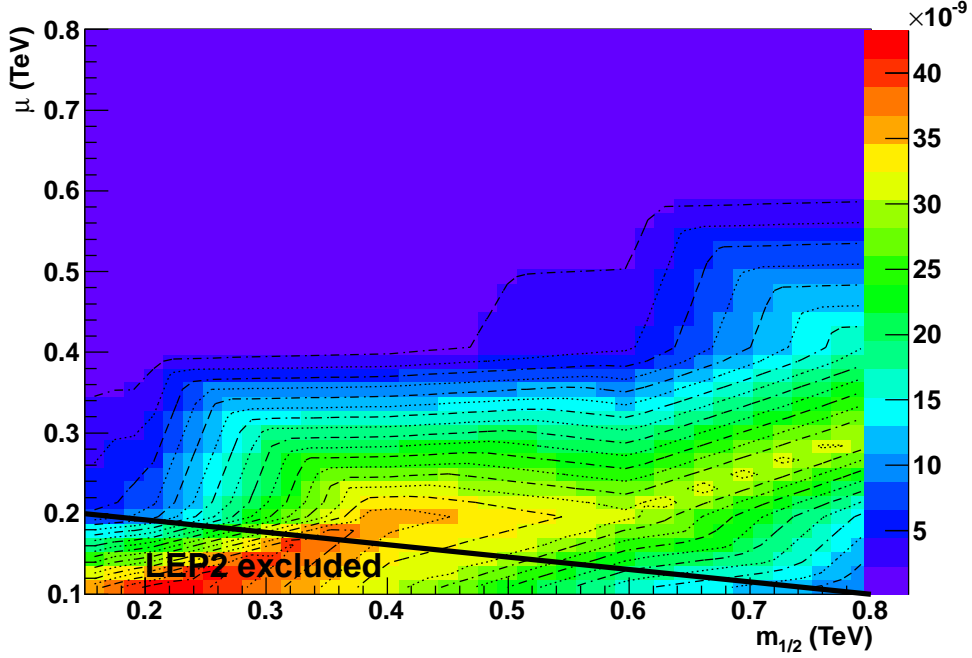


Figure 5: Contours of $\sigma^{SI}(\tilde{Z}_1 p)$ in units of 10^{-9} pb in the μ vs. $m_{1/2}$ plane with $m_A = 800$ GeV, $m_0 = 5000$ GeV, $A_0 = 0$ and $\tan \beta = 10$.

4. Higgsino-world scenario at the LHC

4.1 Sparticle production at LHC7

In the HW scenario, squarks and sleptons are assumed decoupled from collider physics. In the limit of large scalar masses, the reach of LHC7[31] with 2 fb^{-1} for gluino pair production is to $m_{1/2} \sim 250$ GeV (corresponding to $m_{\tilde{g}} \sim 700$ GeV), while the reach of LHC14 with 100 fb^{-1} is to $m_{1/2} \sim 650$ GeV (corresponding to $m_{\tilde{g}} \sim 1400$ GeV)[32]. Thus, for most of HW parameter space, gluino pair production will be below LHC sensitivity. We then expect chargino/neutralino pair production to be the most promising SUSY cross sections at LHC.

In Fig. 7, we show the dominant sparticle pair production cross sections in fb for LHC7 from the higgsino-world scenario versus μ for other model parameters as in Table 1. We adopt the computer code Prospino so that the results are valid at NLO in QCD[33]. For low values of μ , we see that $\tilde{W}_1^\pm \tilde{Z}_1$ and $\tilde{W}_1^\pm \tilde{Z}_2$ are dominant, followed closely by $\tilde{W}_1^+ \tilde{W}_1^-$ and $\tilde{Z}_1 \tilde{Z}_2$ production. As μ moves beyond 300 GeV, the lighter charginos and neutralinos become mixed gaugino-higgsino states, and some of the cross sections drop rapidly. Other potentially visible cross sections such as $\tilde{Z}_2 \tilde{Z}_2$ are several orders of magnitude below these. The sum total of the reactions shown in Fig. 7 agrees well with output for all SUSY reactions as generated by Isajet as shown in Table 1, so these are indeed the dominant production reactions.

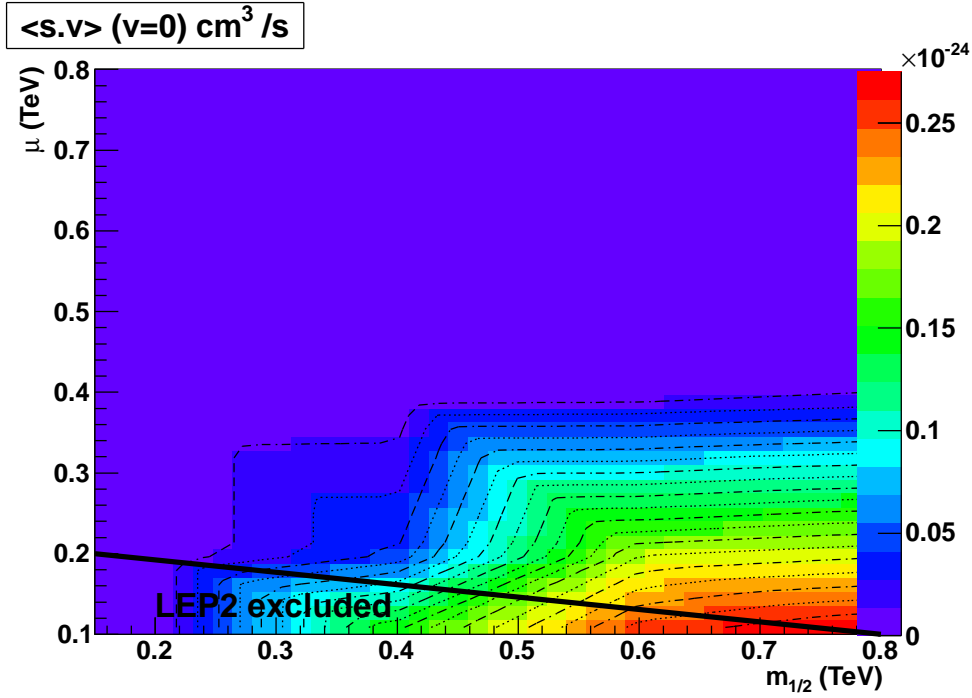


Figure 6: Contours of $\langle \sigma v \rangle|_{v \rightarrow 0}$ in units of $10^{-24} \text{ cm}^3/\text{sec}$ in the μ vs. $m_{1/2}$ plane with $m_A = 800$ GeV, $m_0 = 5000$ GeV, $A_0 = 0$ and $\tan \beta = 10$.

4.2 Branching fractions and collider signatures

The sparticle branching fractions can be read off from the Isajet decay table for sparticle cascade decays[34]. For light charginos \widetilde{W}_1 , we find

- $\widetilde{W}_1^- \rightarrow \ell \bar{\nu}_\ell \widetilde{Z}_1$ at 11.1% for each species $\ell = e, \mu$ or τ ,
- $\widetilde{W}_1^- \rightarrow d \bar{u} \widetilde{Z}_1$ at 33.3% ,
- $\widetilde{W}_1^- \rightarrow s \bar{c} \widetilde{Z}_1$ at 33.3%

since the three-body chargino decays are dominated by the W^* propagator.

For \widetilde{Z}_2 , we find typically

- $\widetilde{Z}_2 \rightarrow \ell^+ \ell^- \widetilde{Z}_1$ at 3.5% for each species $\ell = e, \mu$ or τ ,
- $\widetilde{Z}_2 \rightarrow \nu_\ell \bar{\nu}_\ell \widetilde{Z}_1$ at 21.5% (summed over all neutrino species) and
- $\widetilde{Z}_2 \rightarrow q \bar{q} \widetilde{Z}_1$ at 68% summed over all quark species.

In addition, the decay $\widetilde{Z}_2 \rightarrow \widetilde{Z}_1 \gamma$ occurs at an enhanced rate: 0.8% (0.2%) for HW150 (HW300)[35].

By combining production cross sections with branching fractions, we find that $\widetilde{W}_1 \widetilde{Z}_1$ production will lead to either soft jets+MET (likely buried under QCD background(BG)) or a soft isolated lepton+MET (likely buried under BG from direct W -boson production). Thus, we do not expect this reaction to lead to observable signatures.

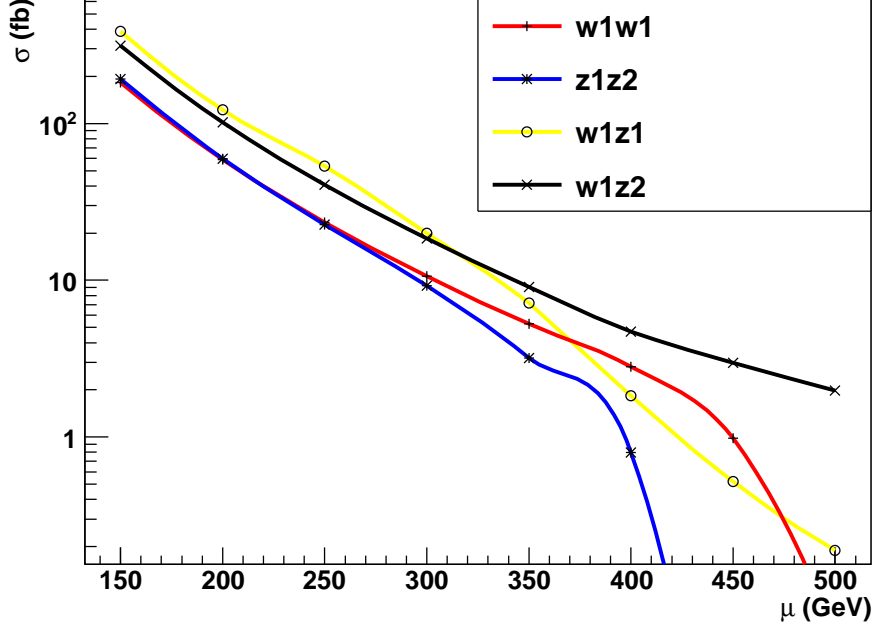


Figure 7: Dominant chargino and neutralino production cross sections versus μ at LHC7 for light higgsino-world SUSY scenario. Other parameters are fixed as in Fig. 1.

The reaction $\widetilde{W}_1^+ \widetilde{W}_1^-$ will lead to either 1) soft jets+MET, 2) soft isolated lepton plus jets+MET or 3) soft dilepton pair+MET. We expect each of these also to be buried beneath SM backgrounds from QCD or vector boson pair production.

The reaction $\widetilde{Z}_1 \widetilde{Z}_2$ production can lead to 1) soft jets+MET or 2) soft, low invariant mass dilepton pairs+MET. The first of these is likely buried beneath QCD background. The second of these has a chance at observability since the $m(\ell^+ \ell^-)$ will be bounded by $m_{\widetilde{Z}_2} - m_{\widetilde{Z}_1}$ and thus lead to a distinctive mass edge upon a continuum background arising from WW or $Z\gamma^*$ production, where $\gamma^* \rightarrow \ell^+ \ell^-$. If the dilepton pair is at high p_T , due to a highly boosted \widetilde{Z}_2 , then we expect the dilepton pair to be highly collimated in opening angle, and to appear rather distinctively compared to known backgrounds.

The reaction $\widetilde{W}_1 \widetilde{Z}_2$ production will lead to either 1) soft jets+MET, 2) soft jets plus collimated soft dilepton+MET or 3) soft trileptons+MET. The first of these is likely buried beneath QCD background. The second is possibly observable, and should be present if the cleaner $\widetilde{Z}_1 \widetilde{Z}_2 \rightarrow \ell^+ \ell^- + MET$ is found. The third case yields the venerable clean trilepton signature which has been evaluated for the Tevatron[29] and LHC[39, 40]. While $W^* \gamma^*$ and $W^* Z^* \rightarrow 3\ell$ backgrounds proved most daunting for the Tevatron, at LHC the dominant background comes from $t\bar{t}$ production[40].

4.3 Collimated dilepton +MET signature from $\widetilde{Z}_1 \widetilde{Z}_2$ production

We first investigate the $pp \rightarrow \widetilde{Z}_1 \widetilde{Z}_2 \rightarrow \ell^+ \ell^- + MET$ signal against the following SM backgrounds:

- W^+W^- production (including $WW \rightarrow \tau^+\tau^-$),
- $t\bar{t}$ production,
- $\gamma^* \rightarrow \ell^+\ell^-$ (Drell-Yan) production,
- $Z + jets$ with $Z \rightarrow \tau^+\tau^-$ (tau pair) production,
- γ^*Z production, where $Z \rightarrow \nu_\ell\bar{\nu}_\ell$ and $\gamma^* \rightarrow \ell^+\ell^-$ or $\tau^+\tau^-$.

We generate sparticle production and decay events at parton level using Isajet[30] in Les Houches Event (LHE) format, and then feed the LHE files into Pythia[41] for initial/final state radiation, hadronization and underlying event. All backgrounds are generated with Pythia except γ^*Z^* which is generated by Madgraph/MadEvent[42]. The collider events are then fed into the PGS toy detector simulation program[43]. Jets are found using an anti- k_T jet finding algorithm with cone size $\Delta R = 0.5$. Leptons are classified as isolated if they contain less than 5 GeV hadronic activity in a cone of $\Delta R = 0.2$ about the lepton direction.

Since the leptons from $\tilde{Z}_1\tilde{Z}_2$ production are expected to be quite soft, we will focus initially upon the case of dimuon production, since muons can be identified more easily than electrons at very low p_T . Signal and background cross sections before and after cuts are listed in Table 2. We first require:

- two opposite-sign muons: one with $p_T(\mu_1) > 15$ GeV and $|\eta(\mu_1)| < 0.9$ (central region), while the other has $p_T(\mu_2) > 5$ GeV with $|\eta(\mu_2)| < 2.4$.

To reduce the large background from Drell-Yan dimuon production, we next impose

- $MET > 25$ GeV,

since MET in the DY case only arises from particles lost along the beam-line or cracks, or from energy mis-measurement, mainly from hadron radiation. There is also a large background from $t\bar{t}$ production of dimuons and a background from single top in association with a W-boson which has a hard b-jet, but this always comes along with two hard b -jets from the $t \rightarrow bW$ decays. Thus, we also require the number of jets

- $n(jets) = 0$,

where jets are identified as a cluster of hadrons with $p_T(jet) > 15$ GeV, $|\eta(jet)| < 2.4$. At this stage, the largest background comes from W^+W^- production, which yields a continuum distribution in dimuon invariant mass $m(\mu^+\mu^-)$, whilst the signal dimuons are restricted to $m(\mu^+\mu^-) < m_{\tilde{Z}_2} - m_{\tilde{Z}_1}$ which is just 16.2 GeV for HW150. Thus, we require

- $m(\mu^+\mu^-) < 20$ GeV .

Signal and BG after these cuts are listed for HW150 in Table 2.

From Table 2, we see that the dimuon signal comes about 30% from $\tilde{Z}_1\tilde{Z}_2$ production, and about 70% from $\tilde{W}_1\tilde{Z}_2$ production. In the latter case, the \tilde{W}_1 usually decays to $q\bar{q}'\tilde{Z}_1$

process	σ (fb)	σ (after cuts, fb)
$\tilde{W}_1 \tilde{Z}_2$	313	0.3
$\tilde{Z}_1 \tilde{Z}_2$	192	0.13
$\gamma^* \rightarrow \mu^+ \mu^-$ (DY)	1.1×10^6	4
$W^+ W^- \rightarrow \mu^+ \mu^-$	235.5	2.3
$\gamma^* Z \rightarrow \mu^+ \mu^- \nu_i \bar{\nu}_i$	6.8	0.3
$\gamma^*, Z \rightarrow \tau^+ \tau^- \rightarrow \mu^+ \mu^-$	1.5×10^4	5
$t\bar{t} \rightarrow \mu^+ \mu^-$	8.9×10^4	< 0.3

Table 2: Signal and BG cross sections in fb before and after cuts at LHC7. The signal rates are for higgsino-world benchmark point HW150. Each background process requires $p_T(\mu) > 5$ GeV.

but with very low energy release, which sometimes escapes the “no-jet” cut. Meanwhile, the dominant remaining background comes from tau-pair, Drell-Yan and $W^+ W^-$ production. The remaining signal is 0.43 fb, while the summed SM background is ~ 11.9 fb. The 5σ discovery cross section for LHC7, assuming 10 fb^{-1} of integrated luminosity is 5.45 fb, so that the case of HW150 is far below this limit.

The inclusive muon p_T distribution before cuts is shown in Fig. 8 for the HW150 benchmark. Here, we see that the spectrum from HW150 benchmark is very soft, with the bulk of the distribution below 15 GeV. Thus, few of the signal events escape even the first cut listed above on $p_T(\mu) > 15$ GeV. The signal rates for HW150 after cuts only corresponds to four events in 10 fb^{-1} of integrated luminosity, while SM background lies at the ~ 120 event level.

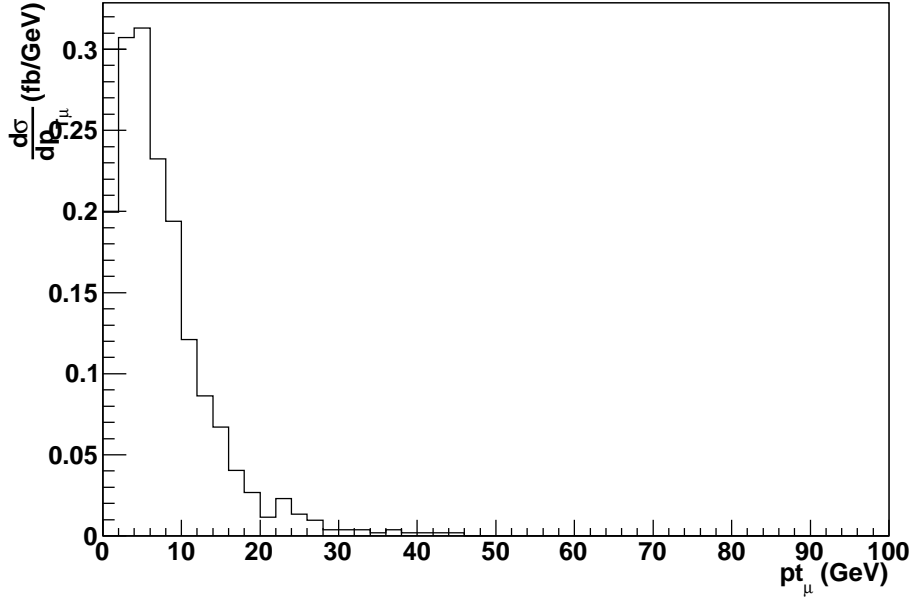


Figure 8: Distribution in $p_T(\mu)$ from $pp \rightarrow \tilde{Z}_1 \tilde{Z}_2 \rightarrow \mu^+ \mu^- + E_T^{\text{miss}}$ events at LHC from higgsino-world benchmark point HW150.

Likewise, trilepton signatures from $\widetilde{W}_1^\pm \widetilde{Z}_2$ production yield a very soft isolated lepton spectrum, and are also difficult to extract at an observable level. The search for jets+ MET from higgsino pair production also yields a very soft jet and MET spectrum, and is difficult to extract from prodigious SM backgrounds.

Thus, higgsino-world SUSY seems capable of eluding standard SUSY searches via isolated multi-leptons. The key feature of the HW scenario is that possibly observable levels of dimuon and trimuon production can occur, but at very low p_T levels. Our studies then motivate our experimental colleagues to push for dimuon and trimuon analyses at the very lowest $p_T(\mu)$ levels in order to extract a possible signal.

5. Prospects for ILC or a muon collider

We have seen that the LHC has essentially no reach for the HW SUSY scenario due to a very soft spectrum of observable particle decay products. However, we have seen that the HW scenario mainly occurs for $\mu \lesssim 250$ GeV (for $m_{1/2} \lesssim 1$ TeV), which also corresponds to $m_{\widetilde{W}_1} \lesssim 250$ GeV. Contours of $2m_{\widetilde{W}_1}$ are shown in Fig. 9, where we see that the region with $2m_{\widetilde{W}_1} \lesssim 500$ GeV covers almost all of HW parameter space (compare against Fig. 2). For this mass range, chargino pair production, and also $\widetilde{Z}_1 \widetilde{Z}_2$ production, should be within range of the proposed international Linear Collider (ILC), which is proposed to operate initially at an energy $\sqrt{s} = 500$ GeV. Chargino pair production would also be accessible to higher energy e^+e^- colliders like CLIC, or a muon collider (MC) operating in the TeV regime.

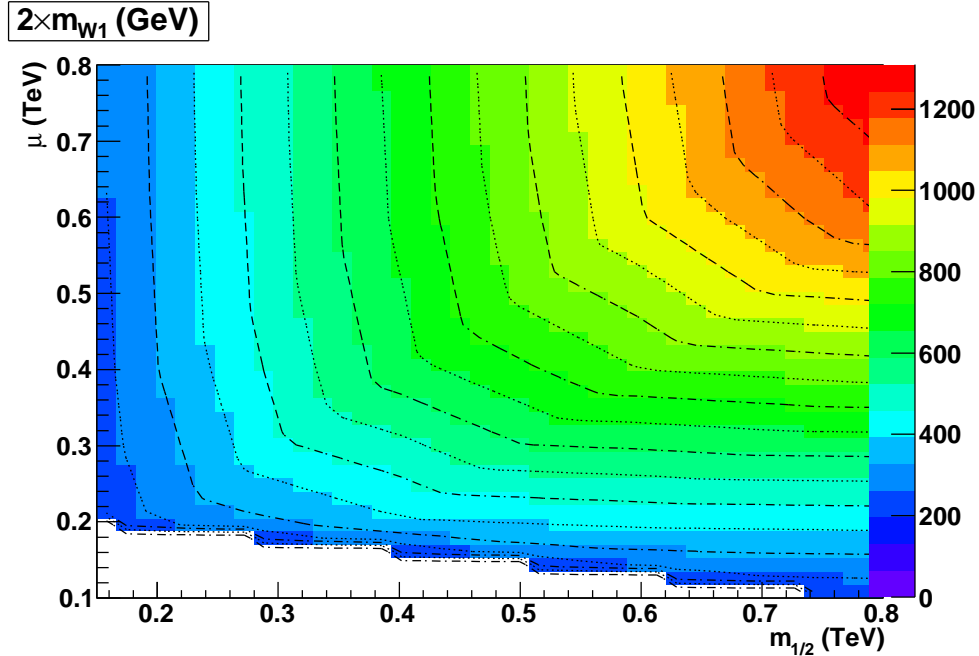


Figure 9: Contours of $2m_{\widetilde{W}_1}$ in the μ versus $m_{1/2}$ parameter plane for other SUSY parameters as in HW150 scenario.

In Fig. 10, we show the cross sections for $e^+e^- \rightarrow \widetilde{W}_1^+\widetilde{W}_1^-$ and $e^+e^- \rightarrow \widetilde{Z}_1\widetilde{Z}_2$ using SUSY parameters as in the HW150 benchmark, but with μ varying from 100-250 GeV. The variation in μ causes $m_{\widetilde{W}_1}$ to vary, and in fact $m_{\widetilde{W}_1} \sim \mu$, so that our results are plotted versus the more physical $m_{\widetilde{W}_1}$ value. We take $\sqrt{s} = 500$ GeV. We see that over most of HW parameter space, the chargino pair production cross section is in the several hundred fb range, until $m_{\widetilde{W}_1}$ approaches the kinematic limit for pair production. Chargino pair production will be signaled at ILC or MC by 1) soft multijet + \cancel{E} production, 2) soft isolated lepton plus jets + \cancel{E} production and 3) dilepton + \cancel{E} production, depending on whether the charginos decay leptonically or hadronically. These signatures should be easily visible against SM backgrounds such as WW production via distributions such as “missing mass”: $\eta = \sqrt{\cancel{E}^2 - \cancel{p}^2}$ [45]. In addition, SM backgrounds such as dilepton or dijet production from the $\gamma\gamma$ initial state will contain energy depositions all in the same plane, while the SUSY signal will contain acoplanar events. Thus, the HW scenario should be easily visible at ILC, or a higher energy muon collider, even though it is difficult to see at LHC.

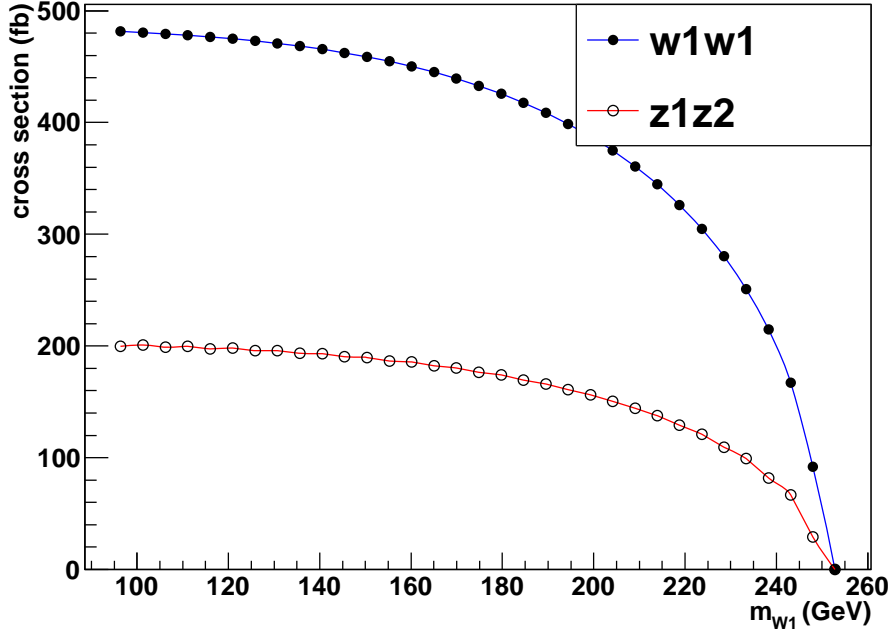


Figure 10: Cross sections for chargino pair production and neutralino pair production versus $m_{\widetilde{W}_1}$ at a $\sqrt{s} = 500$ GeV ILC or MC collider. We take SUSY parameters as in Fig. 7, and vary μ to give variation in $m_{\widetilde{W}_1}$.

A distinctive feature of the HW scenario is that the \widetilde{W}_1 , \widetilde{Z}_1 and \widetilde{Z}_2 are all mainly higgsino-like, whereas in models such as mSUGRA, these states are almost always gaugino-like. In Ref. [45], it is shown that for wino-like \widetilde{W}_1 and \widetilde{Z}_2 , the $\widetilde{W}_1^+\widetilde{W}_1^-$ and $\widetilde{Z}_1\widetilde{Z}_2$ production cross sections are steeply increasing functions of the electron beam polarization $P_L(e^-)$ (where $P_L(e^-) \sim -1$ corresponds to pure right-polarized e^- , $P_L(e^-) = +1$ corresponds

to pure left-polarized e^- , and $P_L(e^-) = 0$ corresponds to unpolarized e^- beams). In Fig. 11, we plot the $e^+e^- \rightarrow \widetilde{W}_1^+\widetilde{W}_1^-$ and $\widetilde{Z}_1\widetilde{Z}_2$ cross sections versus $P_L(e^-)$ for the HW150 benchmark. In the HW scenario, $\widetilde{W}_1^+\widetilde{W}_1^-$ production only increases by a factor of ~ 3.5 as $P_L(e^-)$ varies from -1 to +1, whereas in mSUGRA it typically increases by factors of about 100[45]. In addition, the $\widetilde{Z}_1\widetilde{Z}_2$ cross section for HW150 is nearly flat versus $P_L(e^-)$, while in mSUGRA, it is typically increasing by factors of 20-30. Thus, variability of the SUSY production cross sections versus beam polarization will quickly allow one to extract much of the gaugino/higgsino content of the charginos/neutralinos which are accessible to an ILC with adjustable beam polarization.

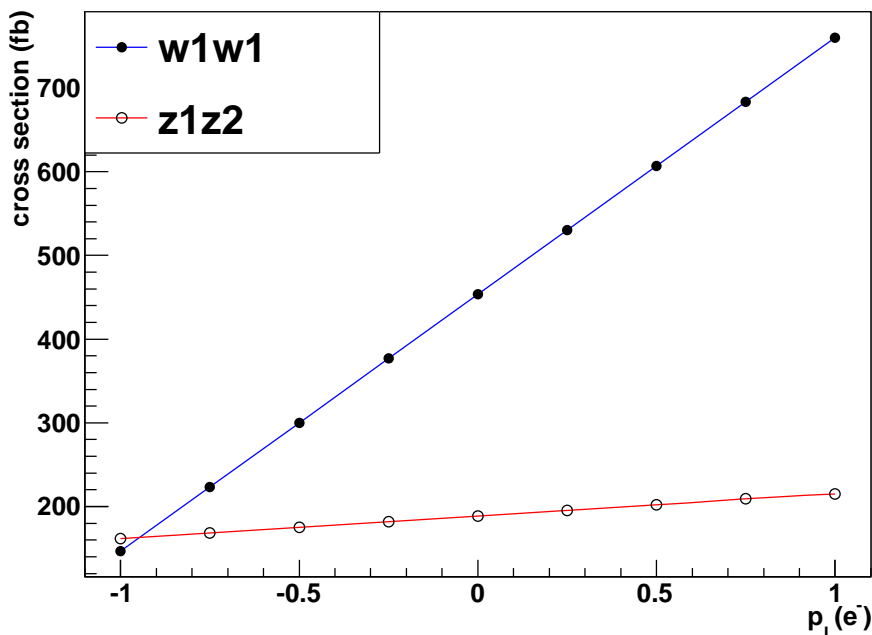


Figure 11: Cross sections for chargino pair production and neutralino pair production versus $P_L(e^-)$ at a $\sqrt{s} = 500$ GeV ILC collider. We take SUSY parameters as in HW1, with $\mu = 150$ GeV.

6. Summary and conclusions

The higgsino-world SUSY scenario with multi-TeV scalars, $\mu \lesssim 250$ GeV and intermediate scale gauginos is very appealing in that it can reconcile a decoupling solution to the SUSY flavor, CP, p -decay and gravitino problems with apparently low levels of naturalness or electroweak fine-tuning. The scenario is characterized by a mass hierarchy $|\mu| \ll m_{1/2} \ll m_0$, where m_0 is the GUT scale mass of matter scalars. The HW scenario is most easily realized in models with non-universal Higgs masses, where the weak scale values of μ and m_A are taken as free parameters. In the HW scenario, the \widetilde{W}_1 , \widetilde{Z}_1 and \widetilde{Z}_2 states are all light with mass $\lesssim 250$ GeV, and dominantly higgsino-like. The remaining sparticles may well be heavy and inaccessible to LHC searches.

The standard thermal abundance of higgsino-like \tilde{Z}_1 particles is well below WMAP-measured values. However, in appealing cosmological scenarios such as those containing TeV-scale scalar fields such as moduli, or in scenarios with mixed axion- \tilde{Z}_1 cold dark matter, the neutralino abundance can be easily pushed up into the measured range. If this is so, then there are excellent prospects for direct or indirect detection of higgsino-like relic WIMPs, and we expect experiments such as Xenon-100 or Xenon-1-ton to fully explore this possibility. Alternatively, in DM models such as the mixed $a\tilde{Z}_1$ scenario[24], it is also possible to tune PQ parameters such that the WIMP abundance remains tiny, while the bulk of CDM is comprised of axions. Thus, the HW scenario will not be completely excludable by direct or indirect WIMP search experiments if no signals for WIMPs are seen.

At the LHC, gluino and squark production may be suppressed by large values of $m_{\tilde{g}}$ and especially $m_{\tilde{q}}$. The $\tilde{W}_1\tilde{Z}_1$, $\tilde{W}_1\tilde{Z}_2$, $\tilde{Z}_1\tilde{Z}_2$ and $\tilde{W}_1^+\tilde{W}_1^-$ production reactions are then dominant, but are difficult to detect at LHC due to the small $\tilde{W}_1 - \tilde{Z}_1$ and $\tilde{Z}_2 - \tilde{Z}_1$ mass gaps, which lead to very soft visible particle production. The reaction $pp \rightarrow \tilde{Z}_1\tilde{Z}_2$ may lead to tightly collimated OS/SF dilepton pairs, although calculations of signal and background after simple cuts indicate these occur at unobservable levels. Trileptons from $\tilde{W}_1\tilde{Z}_2$ production are also difficult to see due to the soft spectrum of isolated leptons. Our studies should motivate our experimental colleagues to push for di- and tri-muon analyses at the very lowest levels of $p_T(\mu)$ which are possible.

A linear e^+e^- collider such as ILC or a $\mu^+\mu^-$ collider operating with $\sqrt{s} \sim 0.5 - 1$ TeV should be able to make a thorough search for the HW scenario. If HW SUSY is discovered at ILC, then it should be possible to extract the gaugino/higgsino content of the \tilde{W}_1 , \tilde{Z}_2 and \tilde{Z}_1 states using various kinematic and angular distributions along with beam polarization. Thus, the HW scenario provides a concrete realization of a SUSY construct which may well remain hidden from LHC and dark matter searches, but which is fully testable at a TeV-scale lepton collider.

Acknowledgments

This work was supported in part by the U.S. Department of Energy under grant No. DE-FG02-04ER41305 and DE-FG02-95ER40896. VB thanks the KITP-Santa Barbara for its hospitality.

References

- [1] The Minimal Supersymmetric Standard Model commonly used today was introduced by, S. Dimopoulos and H. Georgi, *Nucl. Phys.* **B 193** (1981) 150; N. Sakai, *Z. Physik* **C 11** (1981) 153; for reviews of SUSY phenomenology, see H. Baer and X. Tata, *Weak Scale Supersymmetry: From Superfields to Scattering Events*, (Cambridge University Press, 2006); M. Drees, R. Godbole and P. Roy, *Theory and Phenomenology of Sparticles*, (World Scientific, 2004); P. Binetruy, *Supersymmetry* (Oxford University Press, 2006); S. P. Martin, hep-ph/9709356.

- [2] F. Gabbiani, E. Gabrielli, A. Masiero and L. Silvestrini, *Nucl. Phys. B* **477** (1996) 321 [arXiv:hep-ph/9604387].
- [3] H. Murayama and A. Pierce, *Phys. Rev. D* **65** (2002) 055009 [arXiv:hep-ph/0108104].
- [4] S. Weinberg, *Phys. Rev. Lett.* **48** (1982) 1303, M. Khlopov and A. Linde, *Phys. Lett. B* **138** (1984) 265.
- [5] M. Fukugita and T. Yanagida, *Phys. Lett. B* **174** (1986) 45; M. Luty, *Phys. Rev. D* **45** (1992) 455; W. Buchmüller and M. Plumacher, *Phys. Lett. B* **389** (1996) 73 and *Int. J. Mod. Phys. A* **15** (2000) 5047; R. Barbieri, P. Creminelli, A. Strumia and N. Tetradis, *Nucl. Phys. B* **575** (2000) 61; G. F. Giudice, A. Notari, M. Raidal, A. Riotto and A. Strumia, *Nucl. Phys. B* **685** (2004) 89; for a recent review, see W. Buchmüller, R. Peccei and T. Yanagida, *Ann. Rev. Nucl. Part. Sci.* **55** (2005) 311; W. Buchmüller, P. Di Bari and M. Plumacher, *Nucl. Phys. B* **643** (2002) 367 and Erratum-ibid, **B793** (2008) 362; *Annals Phys.* **315** (2005) 305 and *New J. Phys.* **6** (2004) 105.
- [6] G. Lazarides and Q. Shafi, *Phys. Lett. B* **258** (1991) 305; K. Kumeekawa, T. Moroi and T. Yanagida, *Prog. Theor. Phys.* **92** (1994) 437; T. Asaka, K. Hamaguchi, M. Kawasaki and T. Yanagida, *Phys. Lett. B* **464** (1999) 12; G. F. Giudice, M. Peloso, A. Riotto and I. Tkachev, *J. High Energy Phys.* **9908** (1999) 014.
- [7] M. Dine, A. Kagan and S. Samuel, *Phys. Lett. B* **243** (1990) 250; A. Cohen, D. B. Kaplan and A. Nelson, *Phys. Lett. B* **388** (1996) 588; H. Baer, S. Kraml, A. Lessa, S. Sekmen and X. Tata, *JHEP* **1010** (2010) 018
- [8] M. Y. Khlopov and A. Linde, *Phys. Lett. B* **138** (1984) 265; for an update, see M. Kawasaki, K. Kohri, T. Moroi and A. Yotsuyanagi, *Phys. Rev. D* **78** (2008) 065011.
- [9] H. Baer and X. Tata, *Weak Scale Supersymmetry: From Superfields to Scattering Events*, (Cambridge University Press, 2006).
- [10] R. Barbieri and G. Giudice,
- [11] G. W. Anderson and D. J. Castano, *Phys. Lett. B* **347** (1995) 300 [arXiv:hep-ph/9409419].
- [12] K. L. Chan, U. Chattopadhyay and P. Nath, *Phys. Rev. D* **58** (1998) 096004.
- [13] J. Feng, K. Matchev and T. Moroi, *Phys. Rev. Lett.* **84** (2000) 2322 and *Phys. Rev. D* **61** (2000) 075005.
- [14] G. L. Kane, In **Kane, G.L. (ed.): Perspectives on supersymmetry** 352-354; G. Kane and J. Wells, *Phys. Rev. Lett.* **76** (1996) 4458.
- [15] E. Komatsu *et al.* (WMAP collaboration), arXiv:1001.4538 (2010).
- [16] J. Ellis and K. Olive, *Phys. Lett. B* **514** (2001) 114; H. Baer and A. Box, *Eur. Phys. J. C* **68** (2010) 523; H. Baer, A. Box and H. Summy, *J. High Energy Phys.* **1010** (2010) 023
- [17] B. Acharya, G. Kane, S. Watson and P. Kumar, *Phys. Rev. D* **80** (2009) 083529.
- [18] T. Moroi and L. Randall, *Nucl. Phys. B* **570** (2000) 455.
- [19] G. Gelmini and P. Gondolo, *Phys. Rev. D* **74** (2006) 023510; G. Gelmini, P. Gondolo, A. Soldatenko and C. Yaguna, *Phys. Rev. D* **74** (2006) 083514.
- [20] R. Peccei and H. Quinn, *Phys. Rev. Lett.* **38** (1977) 1440 and *Phys. Rev. D* **16** (1977) 1791; S. Weinberg, *Phys. Rev. Lett.* **40** (1978) 223; F. Wilczek, *Phys. Rev. Lett.* **40** (1978) 279.

- [21] J. E. Kim, *Phys. Rev. Lett.* **43** (1979) 103; M. A. Shifman, A. Vainshtein and V. I. Zakharov, *Nucl. Phys.* **B 166** (1980) 493.
- [22] M. Dine, W. Fischler and M. Srednicki, *Phys. Lett.* **B 104** (1981) 199; A. P. Zhitnitskii, *Sov. J. Nucl.* **31** (1980) 260.
- [23] K-Y. Choi, J. E. Kim, H. M. Lee and O. Seto, *Phys. Rev.* **D 77** (2008) 123501.
- [24] H. Baer, A. Lessa, S. Rajagopalan and W. Sreethawong, *JCAP***1106** (2011) 031.
- [25] M. Bolz, A. Brandenburg and W. Buchmuller, *Nucl. Phys.* **B 606** (2001) 518; J. Pradler and F. Steffen, *Phys. Rev.* **D 75** (2007) 023509; V. S. Rychkov and A. Strumia, *Phys. Rev.* **D 75** (2007) 075011.
- [26] K. Kohri, M. Yamaguchi and J. Yokoyama, *Phys. Rev.* **D 72** (2005) 083510; T. Asaka, S. Nakamura and M. Yamaguchi, *Phys. Rev.* **D 74** (2006) 023520; M. Endo, F. Takahashi and T. T. Yanagida, *Phys. Rev.* **D 76** (2007) 083509.
- [27] H. Baer, R. Dermisek, S. Rajagopalan and H. Summy, *JCAP***1007** (2010) 014.
- [28] J. Ellis, K. Olive and Y. Santoso, *Phys. Lett.* **B 539** (2002) 107; J. Ellis, T. Falk, K. Olive and Y. Santoso, *Nucl. Phys.* **B 652** (2003) 259; H. Baer, A. Mustafayev, S. Profumo, A. Belyaev and X. Tata, *Phys. Rev.* **D 71** (2005) 095008 and *J. High Energy Phys.* **0507** (2005) 065, and references therein.
- [29] H. Baer and X. Tata, *Phys. Rev.* **D 47** (1993) 2739; H. Baer, M. Drees, F. Paige, P. Quintana and X. Tata, *Phys. Rev.* **D 61** (2000) 095007; V. Barger and C. Kao, *Phys. Rev.* **D 60** (1999) 115015 and K. Matchev and D. Pierce, *Phys. Lett.* **B 467** (1999) 225. For a review, see S. Abel *et al.* [hep-ph/0003154](#).
- [30] ISAJET, by H. Baer, F. Paige, S. Protopopescu and X. Tata, [hep-ph/0312045](#); see also H. Baer, J. Ferrandis, S. Kraml and W. Porod, *Phys. Rev.* **D 73** (2006) 015010.
- [31] H. Baer, V. Barger, A. Lessa and X. Tata, *J. High Energy Phys.* **1006** (2010) 102.
- [32] H. Baer, X. Tata and J. Woodside, *Phys. Rev.* **D 45** (1992) 142; H. Baer, C. H. Chen, F. Paige and X. Tata, *Phys. Rev.* **D 52** (1995) 2746 and *Phys. Rev.* **D 53** (1996) 6241; H. Baer, C. H. Chen, M. Drees, F. Paige and X. Tata, *Phys. Rev.* **D 59** (1999) 055014; H. Baer, C. Balázs, A. Belyaev, T. Krupovnickas and X. Tata, *J. High Energy Phys.* **0306** (2003) 054; see also, S. Abdullin and F. Charles, *Nucl. Phys.* **B 547** (1999) 60; S. Abdullin *et al.* (CMS Collaboration), *J. Phys.* **G 28** (2002) 469 [[hep-ph/9806366](#)]; B. Allanach, J. Hetherington, A. Parker and B. Webber, *J. High Energy Phys.* **08** (2000) 017.
- [33] W. Beenakker, R. Hopker, M. Spira, [hep-ph/9611232](#) (1996).
- [34] H. Baer, J. Ellis, G. Gelmini, D. V. Nanopoulos and X. Tata, *Phys. Lett.* **B 161** (1985) 175; G. Gamberini, *Z. Physik* **C 30** (1986) 605; H. Baer, V. Barger, D. Karatas and X. Tata, *Phys. Rev.* **D 36** (1987) 96.
- [35] H. Baer and T. Krupovnickas, *J. High Energy Phys.* **0209** (2002) 038.
- [36] E Aprile *et al.* (Xenon-100 Collaboration), [arXiv:1104.2549](#) (2011).
- [37] H. Baer, A. Belyaev, T. Krupovnickas and J. O’Farrill, *JCAP***0408** (2004) 005; H. Baer, E. K. Park and X. Tata, *New J. Phys.* **11** (2009) 105024.

- [38] K. Rajagopal, M. Turner and F. Wilczek, *Nucl. Phys.* **B 358** (1991) 447; L. Covi, J. E. Kim and L. Roszkowski, *Phys. Rev. Lett.* **82** (1999) 4180; L. Covi, H. B. Kim, J. E. Kim and L. Roszkowski, *J. High Energy Phys.* **0105** (2001) 033; H. Baer, A. Box and H. Summy, *J. High Energy Phys.* **0908** (2009) 080; for a recent review of axion/axino dark matter, see F. Steffen, arXiv:0811.3347 (2008).
- [39] H. Baer, C. H. Chen, F. Paige and X. Tata, *Phys. Rev.* **D 50** (1994) 4508 and *Phys. Rev.* **D 53** (1996) 6241.
- [40] H. Baer, T. Krupovnickas, S. Profumo and P. Ullio, *J. High Energy Phys.* **0510** (2005) 020.
- [41] T. Sjostrand, S. Mrenna and P. Skands, *J. High Energy Phys.* **0605** (2006) 026.
- [42] J. Alwall, M. Herquet, F. Maltoni, O. Mattelaer and T. Stelzer, *JHEP* **1106** (2011) 128.
- [43] J. Conway, PGS,
<http://physics.ucdavis.edu/~conway/research/software/pgs/pgs4-general.htm>
- [44] H. Baer, K. Hagiwara and X. Tata, *Phys. Rev.* **D 35** (1987) 1598; H. Baer, D. Dzialo-Karatas and X. Tata, *Phys. Rev.* **D 42** (1990) 2259; H. Baer, C. Kao and X. Tata, *Phys. Rev.* **D 48** (1993) 5175; H. Baer, C. H. Chen, F. Paige and X. Tata, *Phys. Rev.* **D 50** (1994) 4508; I. Hinchliffe *et al.* *Phys. Rev.* **D 55** (1997) 5520; H. Bachacou, I. Hinchliffe and F. Paige, *Phys. Rev.* **D 62** (2000) 015009; See also, ATLAS collaboration, *Atlas Physics and Detector Performance Technical Design Report* LHCC 99-14/15, and *Expected Performance of the ATLAS Experiment: Detector, Trigger and Physics*, CERN-OPEN-2008-020; CMS Collaboration, *Physics Technical Design Report*, V. II, CERN/LHCC 2006-021.
- [45] H. Baer, R. Munroe and X. Tata, *Phys. Rev.* **D 54** (1996) 6735; H. Baer, A. Belyaev, T. Krupovnickas and X. Tata, *J. High Energy Phys.* **0402** (2004) 007.